

## Immunochemical Determination of 2,4,6-Trichloroanisole as the Responsible Agent for the Musty Odor in Foods. 1. Molecular Modeling Studies for Antibody Production

NURIA SANVICENS, FRANCISCO SÁNCHEZ-BAEZA, AND M.-PILAR MARCO\*

Department of Biological Organic Chemistry, IIQAB-CSIC, Jordi Girona, 18-26,  
08034-Barcelona, Spain

Nine antisera have been raised against 2,4,6-trichloroanisole (2,4,6-TCA) by immunizing them with three different haptens. With the spacer arm at the *meta* position, hapten **A** (3-(2,4,6-trichloro-3-methoxyphenyl)propanoic acid) preserved all of the functional groups of the target analyte. In hapten **B** (5-(2,4,6-trichlorophenoxy)pentanoic acid), the spacer was placed in the molecule substituting the methoxy group. Finally, hapten **C** (3-(3,5-dichloro-4-methoxyphenyl)propanoic acid) held the spacer arm at the *para* position instead of the chlorine atom of the target analyte. Using theoretical models, we have studied how the molecular geometry and the electronic distribution are affected by the introduction of the linker. The evaluation of the avidity of the resulting antibodies demonstrates that the orientation produced by the spacer arm must also be considered an essential aspect. The screening for competitive assays performed after synthesizing a battery of heterologous competitors has provided with these antibodies eight indirect enzyme-linked immunosorbent assays with acceptable properties. From the number of assays obtained, their maximal absorbance, their signal-to-noise ratio, the slope, and the IC<sub>50</sub> values obtained, it can be concluded that hapten **C** provided the best antibodies.

**KEYWORDS:** Trichloroanisole; hapten design; molecular modeling; musty odor; wine; cork; immunoassay

### INTRODUCTION

Cork has been traditionally used to prepare stoppers as closures of champagne and wine bottles due to its peculiar features (impermeability to air and liquids, ability to adhere to glass surface, compressibility, resilience, and chemical inertness) and its recognized positive influence in the wine and champagne aromas. However, the use of cork stoppers has been associated with an undesirable musty and moldy odor known as “cork taint”. In the early 1980s, 2,4,6-trichloroanisole (2,4,6-TCA) was reported to be the primary compound responsible for cork taint in wine (1). Although other compounds, especially other chloroanisoles, can contribute to the musty/earthy odor in wine (2, 3), 2,4,6-TCA has been shown to have the lowest sensory threshold, which varies from 4 to 10 ng L<sup>-1</sup> in white wine and 50 ng L<sup>-1</sup> in red wine (1, 2, 4, 5). Cork taint has become a significant economic problem. It has been estimated that 2–5% of the wine bottles are affected, leading to nearly \$1 billion in losses per year in the wine industry (6).

During the last two decades, many studies have been performed in order to obtain a good understanding of the nature and causes of the cork taint. The compounds associated with this taint, including 2,4,6-TCA, are microbial metabolites produced by naturally occurring microflora present on the cork

oak bark and in the stoppers throughout their production, storage, and transportation (7). One of the most accepted hypotheses points to their formation from chlorophenols, after microorganism detoxification processes occurring through methylation of the phenolic group (8, 9). Chlorophenols have been used for many decades as insecticides and wood and textile preservatives but can also appear after the degradation of other biocides frequently used in the past, such as lindane and hexachlorobenzene (6), or as a consequence of bleaching processes using chlorinating agents (6, 10). In fact, chlorophenols and chloroanisoles residues have been found not only in wine but also in water, sediments, and several food products (11–15). Particularly, pentachlorophenol (PCP), commercialized in Europe as Raco, has been applied for many years on the cork oak base to control insect plagues (16) and the formulation of this product contained not only PCP but also 2,3,4,6-tetrachlorophenol and 2,4,6-trichlorophenol (2,4,6-TCP). It has similarly been speculated that chlorophenols also present in the cellar environment or in the pallets where the wine bottles are stored could be absorbed by the cork and metabolized to TCA by the corresponding microorganisms (3, 17).

The analytical determination of 2,4,6-TCA in liquid media and cork material has relied on chromatographic techniques such as gas chromatography/mass spectrometry (GC/MS) or GC with electron capture detector (5, 7, 10, 18). However, cleanup/preconcentration steps consisting of liquid–liquid extraction

\* To whom correspondence should be addressed. Tel: +34 93 400 6171. Fax: +34 93 204 5904. E-mail: mpmqob@iiqab.csic.es.

with organic solvents followed by solid phase extraction procedures are always required. Moreover, because of the intrinsic volatility of the TCA and its ability to adsorb to the solid surfaces, no agreement has been achieved regarding the efficiency of the TCA extraction procedures (2). In the last years, other approaches that may improve the reliability of the TCA analysis have been evaluated such as solid phase microextraction (19, 20) or supercritical fluid extraction (21). However, high-throughput screening (HTS) methods based on economically attainable and straightforward technologies are required for the small and medium wine and cork producer companies. In this context, immunochemical techniques could not only afford the necessary detectability and specificity for the target analyte with little sample pretreatment but also offer other advantages such as their reliability, simplicity, and low cost (22–28). Moreover, immunochemical techniques can easily be adapted to the simultaneous analysis of many samples, constituting excellent HTS methods.

Immunochemical methods are based on selective antibodies binding to the target analyte. The production of antibodies to low weight molecules, such as TCA, implies the preparation of derivatives named haptens, which have to be coupled to larger molecules in order to raise immunogenicity. The preparation of optimum haptens as immunogens and competitors has been regarded as the most crucial step in the development of an immunochemical technique for small molecules. Many literature examples prove that an appropriate hapten design determines the features of the resulting antibodies, which mainly govern the specificity and the selectivity of an immunochemical technique (22, 29–33). Theoretical molecular models and calculations can be useful tools to assist prediction of which hapten will be the most appropriate to raise antibodies (34–36). Similarly, they can be used to assess the influence of the degree of heterology between the competitors and the analyte (37, 38). With these precedents, in the present paper, we report the studies made to rationalize the effect of the immunizing hapten chemical structure on the features of the resulting immunoassays against TCA.

## EXPERIMENTAL SECTION

**Chemistry. General Methods and Instruments.** Thin-layer chromatography (TLC) was performed on 0.25 mm, precoated silica gel 60 F254 aluminum sheets (Merck, Darmstadt, Germany). Unless otherwise indicated, purification of the reaction mixtures was accomplished by “flash” chromatography using silica gel as the stationary phase.  $^1\text{H}$  and  $^{13}\text{C}$  NMR spectra were obtained with a Varian Unity-300 (Varian Inc., Palo Alto, CA) spectrometer (300 MHz for  $^1\text{H}$  and 75 MHz for  $^{13}\text{C}$ ) or on a Gemini 200 (199.975 MHz for  $^1\text{H}$  and 50.289 for  $^{13}\text{C}$ ). Infrared spectra were measured on a Bomen MB 120 FTIR spectrophotometer (Hartmann & Braun, Québec, Canada). GC/MS was performed on a MD-800 capillary gas chromatograph with an MS quadrupole detector (Fison Instruments, VG, Manchester, U.K.), and the data are reported as  $m/z$  (relative intensity). The ion-source temperature was set at 200 °C, and a 15 m  $\times$  0.25 mm i.d.  $\times$  0.15 mm (film thickness) DB-225 fused capillary column (J&W, Folsom, CA) was used. He was the carrier gas employed at 1 mL/min. GC conditions were as follows: temperature program, 80–220 °C (10 °C/min), 220 °C (10 min); injector temperature, 250 °C.

**Molecular Modeling and Theoretical Calculations.** Molecular modeling was performed using the Hyperchem 4.0 software package (Hypercube Inc, Gainesville, FL). Theoretical geometries and electronic distributions were evaluated for 2,4,6-TCA and potential haptens using semiempirical quantum mechanics MNDO (39) and PM3 (40) models. All of the calculations were performed using standard computational chemistry criteria.

**Synthesis of the Haptens.** The preparation of the haptens **C1**, 2,4,6-trichlorophenoxyacetic acid; **C2**, 2,4,5-trichlorophenoxyacetic acid; **C3**,

4-chloro-methylphenoxyacetic acid; **C4**, 3-chlorophenoxyacetic acid; **C5**, 3-(2-hydroxy-3,5,6-trichlorophenyl)-2-propenoic acid; **C7**, 3-(3-hydroxy-2,4,6-trichlorophenyl)propanoic acid; **C8**, 3-(2-hydroxy-3,5,6-trichlorophenyl)propanoic acid; **C13**, 3-(4-hydroxy-3,5-dichlorophenyl)propanoic acid; **C14**, 3-(2-hydroxy-3,6-dichlorophenyl)propanoic acid; **C15**, 2,6-dichloro-3-hydroxyacetic acid; **C16**, 2,4-dichloro-5-hydroxyacetic acid; and **C21**, 3-hydroxy-2,4,6-trichlorophenylacetic acid has already been reported (36, 37, 41). Hapten **C6**, 2-hydroxy-3,5,6-trichlorobenzoic acid, as well as other chemical reagents were obtained from Aldrich Chemical Co. (Milwaukee, WI). The synthesis of the haptens **A**, **B**, and **C** is described below. The synthesis and the spectral data of the haptens **C9**, **C10**, **C12**, **C18–C20**, and **C22** are given as Supporting Information. The chemical structures of the immunizing and competitor haptens are shown in **Figure 1**.

**3-(2,4,6-Trichloro-3-methoxyphenyl)propanoic Acid (3, Hapten A) General Protocol.** A mixture of  $\text{CH}_3\text{I}$  (0.5 mL, 7.2 mmol) and dry  $\text{K}_2\text{CO}_3$  (0.975 g, 7.2 mmol) was added to a solution of the ester **1** (methyl 3-(3-hydroxy-2,4,6-trichlorophenyl)propanoate) (36) (0.50 g, 1.8 mmol) in anhydrous dimethylformamide (DMF) (7 mL) at room temperature under Ar atmosphere. The mixture was stirred for 12 h at room temperature, washed with  $\text{H}_2\text{O}$  to eliminate the excess of  $\text{CH}_3\text{I}$ , and extracted with  $\text{Et}_2\text{O}$ . The organic layer was then washed again with water and aqueous 1 N HCl to eliminate the remaining DMF. Finally, the resulting organic phase was dried with  $\text{MgSO}_4$ , filtered, and evaporated under reduced pressure. The crude product was purified by column chromatography (silica gel,  $\text{CH}_2\text{Cl}_2$ :hexane 1:1) to obtain the pure anisole **2** as a white solid (0.38 g, 72% yield). Methyl 3-(3-methoxy-2,4,6-trichlorophenyl)propanoate (**2**): IR  $\nu$  (KBr,  $\text{cm}^{-1}$ ): 1745 (C=O), 1458 (COO<sup>-</sup> st), 1176 (C–O st), 865 (ArC–H  $\delta$  oop).  $^1\text{H}$  NMR (200 MHz,  $\text{CDCl}_3$ )  $\delta$  (ppm): 2.56 (t,  $J = 8$  Hz, 2H,  $-\text{CH}_2-\text{COO}-$ ), 3.24 (t,  $J = 8$  Hz, 2H,  $\text{PhCH}_2-$ ), 3.72 (s, 3H,  $-\text{OCH}_3$  ester), 3.88 (s, 3H,  $-\text{OCH}_3$  anisole), 7.36 (s, 1H<sub>Ar</sub>, meta).  $^{13}\text{C}$  NMR (75 MHz,  $\text{CDCl}_3$ )  $\delta$  (ppm): 27.1 ( $-\text{OCH}_3$  ester), 31.7 (C-3), 51.7 (C-2), 60.5 ( $-\text{OCH}_3$  anisole), 127.4 (C-4'), 128.7 (C-2'), 129.8 (C-6'), 130.6 (C-5'), 136.2 (C-1'), 151.4 (C-3'), 172.4 (C-1). EM  $m/z$  (%): 296 ( $\text{M}^+$ , 10), 261 ( $\text{M}^+ - \text{Cl}^+$ , 100), 219 ( $\text{M}^+ - \text{C}_6\text{H}_5^+$ , 88), 159 ( $\text{C}_{10}\text{H}_7\text{O}_2$ , 35), 123 ( $\text{C}_6\text{OCl}$ , 78), 59 ( $\text{C}_2\text{H}_3\text{O}_2$ , 76). Anal. calcd for  $\text{C}_{11}\text{H}_{11}\text{Cl}_3\text{O}_3$ : C, 44.40; H, 3.72; Cl, 35.74. Found: C, 44.57; H, 3.93; Cl, 35.92. Following, the methyl ester was hydrolyzed by dissolving **2** (0.10 g, 0.3 mmol) in tetrahydrofuran (THF, 6 mL) in a round bottom flask provided with a condenser and a magnetic stirrer. A solution of aqueous 1 N NaOH (0.032 g, 0.8 mmol) was added, and the mixture was heated at 80 °C for 3 h. The THF was evaporated, and the crude product was redissolved with a  $\text{NaHCO}_3$  saturated solution (10 mL) and washed with  $\text{Et}_2\text{O}$ . The aqueous phase was then acidified and extracted with  $\text{AcOEt}$ , dried with  $\text{MgSO}_4$ , filtered, and evaporated under reduced pressure to obtain hapten **A** as a white solid (88 mg, 93% yield). IR  $\nu$  (KBr,  $\text{cm}^{-1}$ ): 2939 (COO–H st), 1714 (C=O), 1458 (COO<sup>-</sup> st), 1051 (C–O st), 865 (ArC–H  $\delta$  oop).  $^1\text{H}$  NMR (200 MHz,  $\text{CDCl}_3$ )  $\delta$  (ppm): 2.62 (t,  $J = 8$  Hz, 2H,  $-\text{CH}_2\text{COO}-$ ), 3.26 (t,  $J = 8$  Hz, 2H,  $\text{PhCH}_2-$ ), 3.88 (s, 3H,  $-\text{OCH}_3$ ), 7.37 (s, 1H<sub>Ar</sub>, meta). Melting point, 102–105 °C.

**5-(2,4,6-Trichlorophenoxy)pentanoic Acid (6, Hapten B).** A solution of methyl 5-bromovalerate (0.59 g, 2.5 mmol) in dry acetone (10 mL) was added dropwise to a mixture of 2,4,6-trichlorophenol (**4**) (0.50 g, 2.5 mmol) and dry  $\text{K}_2\text{CO}_3$  (0.96 g, 3.4 mmol) in dry acetone (5 mL) and placed in a round bottom flask provided with a magnetic stirring bar, a Dimroth refrigerant, and a balanced addition funnel under Ar atmosphere. The mixture was heated at 80 °C for 5 h until the disappearance of the starting material by TLC. The solvent was then evaporated, and the remaining crude product was suspended in 1 N HCl (20 mL) and extracted with  $\text{Et}_2\text{O}$  (2  $\times$  30 mL). The organic layer was then washed with a saturated solution of NaCl, dried with  $\text{MgSO}_4$ , filtered, and evaporated to obtain a crude oil that was purified by silica gel flash chromatography using hexane: $\text{Et}_2\text{O}$  (4:1) as the mobile phase. As a result, the methyl 5-(2,4,6-trichlorophenoxy)pentanoate (**5**) was isolated pure as yellow oil (0.48 g, 61% yield).  $^1\text{H}$  NMR (200 MHz,  $\text{CDCl}_3$ )  $\delta$  (ppm): 1.89 (m, 4H,  $-\text{CH}_2-$ ), 2.43 (t,  $J = 6.8$  Hz, 2H,  $-\text{CH}_2\text{COO}-$ ), 3.69 (s, 3H,  $-\text{OCH}_3$ ), 4.00 (t,  $J = 5.4$  Hz, 2H,  $\text{PhCH}_2-$ ), 7.3 (2, 2H<sub>Ar</sub>, meta).  $^{13}\text{C}$  NMR (75 MHz,  $\text{CDCl}_3$ )  $\delta$  (ppm): 21.3 (C-3), 29.3 (C-4), 33.5 (C-2), 51.4 ( $-\text{OCH}_3$ ), 73.1 (C-5), 128.6 (C-2', C-6'), 129.2 (C-4'), 130.0 (C-3', C-5'), 150.4 (C-1'), 173.7 (C-1). Following,

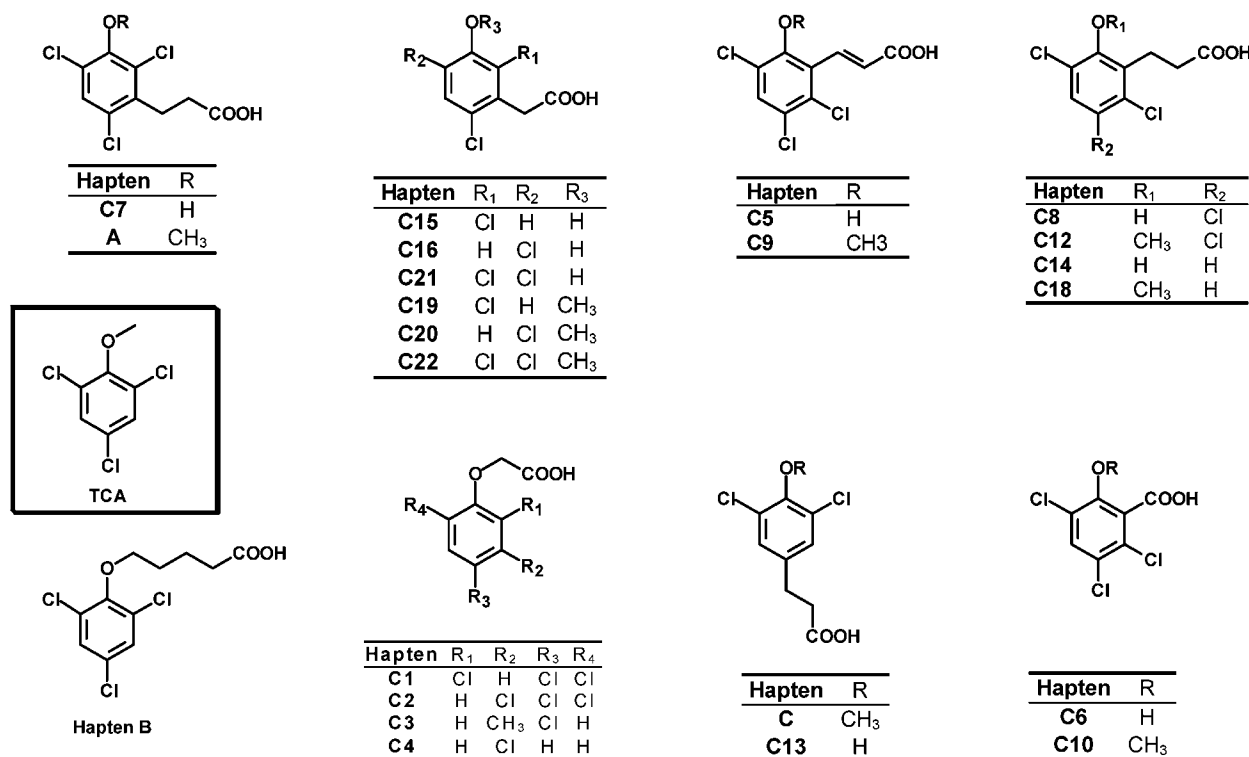


Figure 1. Chemical structures of the immunizing and competitor haptens used throughout this study.

the methyl ester was hydrolyzed as described above by treating the ester **5** (0.1 g, 0.3 mmol) in THF (6 mL) with 1 N NaOH (0.032 g, 0.8 mmol) at 80 °C for 5 h. Finally, hapten **B** was obtained as a white solid (67 mg, 75% yield). IR  $\nu$  (KBr, cm<sup>-1</sup>): 2939 (COO-H st), 1714 (C=O), 1458 (COO<sup>-</sup> st), 1051 (C-O st), 865 (ArC-H  $\delta$  oop). <sup>1</sup>H NMR (200 MHz, CDCl<sub>3</sub>)  $\delta$  (ppm): 1.93 (m, 4H, -CH<sub>2</sub>-), 2.49 (t, *J* = 6.8 Hz, 2H, -CH<sub>2</sub>COO-), 4.01 (t, *J* = 5.4 Hz, 2H, PhCH<sub>2</sub>-), 7.3 (2, 2H<sub>Ar</sub> meta). Melting point, 102–105 °C.

3-(3,5-Dichloro-4-methoxyphenyl)propanoic Acid (**9**, Hapten **C**). From methyl-3-(3,5-dichloro-4-hydroxyphenyl)propanoate (**7**) (**41**), methyl 3-(3,5-dichloro-4-methoxyphenyl)propanoate (**8**) was obtained as a yellow oil (0.5 g, 72% yield). <sup>1</sup>H NMR (300 MHz, CDCl<sub>3</sub>)  $\delta$  (ppm): 2.61 (t, *J* = 7.2 Hz, 2H, -CH<sub>2</sub>COO-), 2.87 (t, *J* = 7.2 Hz, 2H, PhCH<sub>2</sub>-), 3.68 (s, 3H, -OCH<sub>3</sub> ester), 3.87 (s, 3H, -OCH<sub>3</sub> anisole), 6.08 (s, 1H, -OH), 7.14 (s, 2H<sub>Ar</sub> ortho). <sup>13</sup>C NMR (75 MHz, CDCl<sub>3</sub>)  $\delta$  (ppm): 29.8 (-OCH<sub>3</sub> ester), 35.1 (C-3), 51.8 (-OCH<sub>3</sub> anisole), 128.7 (C-3', C-5'), 129.1 (C-2', C-6'), 138.1 (C-1'), 146.3 (C-4'), 172.7 (C-1). The hydrolysis of the ester yielded hapten **C** as a white solid (0.30 g, 71% yield). <sup>1</sup>H NMR (300 MHz, CDCl<sub>3</sub>)  $\delta$  (ppm): 2.66 (t, *J* = 7.8 Hz, 2H, -CH<sub>2</sub>COO-), 2.87 (t, *J* = 7.8 Hz, 2H, PhCH<sub>2</sub>-), 3.88 (s, 3H, -OCH<sub>3</sub> anisole), 7.14 (s, 2H<sub>Ar</sub> ortho). Melting point, 63–65 °C.

**B. Immunochemistry. General Methods and Instruments.** The MALDI-TOF-MS (matrix-assisted laser desorption ionization time-of-flight mass spectrometer) used for analyzing the protein conjugates was a Perspective BioSpectrometry Workstation provided with the software Voyager-DE-RP (version 4.03) developed by Perspective Biosystems Inc. (Framingham, MA) and Grams/386 (for Microsoft Windows, version 3.04, level III) developed by Galactic Industries Corporation (Salem, NH). The pH and the conductivity of all buffers and solutions were measured with a pH meter pH 540 GLP and a conductimeter LF 340, respectively (WTW, Weilheim, Germany). Polystyrene microtiter plates were purchased from Nunc (Maxisorp, Roskilde, DK). Washing steps were performed on a SLY96 PW microplate washer (SLT Labinstruments GmbH, Salzburg, Austria). Absorbances were read on a SpectramaxPlus (Molecular Devices, Sunnyvale, CA). The competitive curves were analyzed with a four parameter logistic equation using the software SoftmaxPro v2.6 (Molecular Devices) and GraphPad Prism (GraphPad Software Inc., San Diego, CA). Unless otherwise indicated, data presented correspond to the average of at least two well replicates.

**Chemicals and Immunochemicals.** Immunochemicals were obtained from Sigma Chemical Co. (St. Louis, MO). The preparation of the protein conjugates and the antisera is described below.

**Buffers.** Unless otherwise indicated, phosphate-buffered saline (PBS) is 0.01 M phosphate buffer and 0.8% saline solution, and the pH is 7.5. PBST is PBS with 0.05% Tween 20. Borate buffer is 0.2 M boric acid-sodium borate, pH 8.7. Coating buffer is 0.05 M carbonate-bicarbonate buffer, pH 9.6. Citrate buffer is a 0.04 M solution of sodium citrate, pH 5.5. The substrate solution contains 0.01% TMB (tetramethylbenzidine) and 0.004% H<sub>2</sub>O<sub>2</sub> in citrate buffer.

**Preparation of the Immunogens and Bovine Serum Albumins (BSA) Homologous Antigens. Active Ester (AE) Method.** Following described procedures (**42**), haptens **A**, **B**, and **C** (60  $\mu$ mol) were reacted with freshly prepared solutions of *N*-hydroxysuccinimide (8.62 mg, 75  $\mu$ mol) and dicyclohexylcarbodiimide (30.90 mg, 150  $\mu$ mol) in anhydrous DMF (200  $\mu$ L) for about 2 h at room temperature until the appearance of the urea precipitate that was removed by centrifugation. The supernatant of each solution was split in two and then added dropwise to a KLH solution and to BSA solution (30 mg/each) in 0.2 M borate buffer (1.8 mL) and stirred for 3 h at room temperature. The protein conjugates were purified by dialysis against 0.5 mM PBS (4  $\times$  5 L) and milliQ water (1  $\times$  5 L) and stored freeze-dried at -40 °C. Unless otherwise indicated, working aliquots were stored at 4 °C in 0.01 M PBS at 1 mg mL<sup>-1</sup>. Hapten densities of the BSA conjugates were determined by MALDI-TOF-MS by comparing the molecular weight of the standard BSA and that of the conjugates (results available as Supporting Information).

**Preparation of the Coating Antigens. Mixed Anhydride (MA) Method.** Following the described procedures (**43**, **44**), the immunizing and competitor haptens (15  $\mu$ mol) were reacted with tributylamine (4  $\mu$ L, 16.5  $\mu$ mol) and isobutylchloroformate (3  $\mu$ L, 18  $\mu$ mol) in DMF (160  $\mu$ L). The solution containing the activated hapten was then divided in three equivalent fractions and added to the BSA, CONA, and OVA (10 mg/each) solutions in 0.2 M borate buffer (1.8 mL). The conjugates were purified as described above. As before, hapten densities of the BSA conjugates were determined by MALDI-TOF-MS (results available as Supporting Information).

**Polyclonal Antisera.** The immunization protocol was performed on female New Zealand white rabbits weighing 1–2 kg, as previously described (**42**). Rabbits 74, 75, and 76 were immunized with A-KLH,

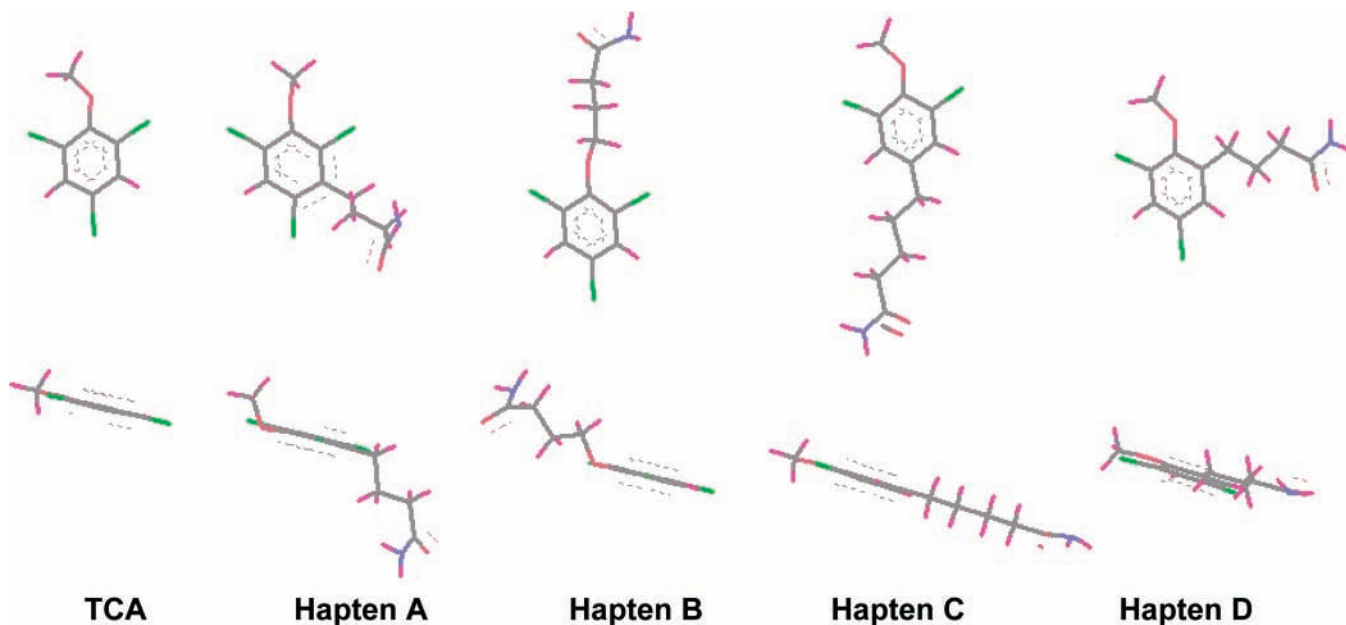


**Figure 2.** MNDO optimized geometries of the target analyte and haptens A–D in frontal (top) and side (bottom) views. Calculations have been made using the corresponding amide derivatives of the haptens. Gray is carbon; green is chlorine; red is oxygen; magenta is hydrogen; and dark blue is nitrogen.

rabbits 77–79 were immunized with **B**-KLH, and rabbits 88–90 were immunized with **C**-KLH. The corresponding antisera (As) obtained were named with the rabbit numbers. Evolution of the antibody titer was assessed by measuring the binding of serial dilutions of the different antisera to microtiter plates coated with **A**-BSA (AE) for As74–76, with **B**-BSA (AE) for As77–79, and with **C**-BSA (AE) for As88–90. After an acceptable antibody titer was observed, the animals were exsanguinated and the blood was collected on vacutainer tubes provided with a serum separation gel. Antisera were obtained by centrifugation and stored at  $-40\text{ }^{\circ}\text{C}$  in the presence of 0.02%  $\text{NaN}_3$ .

**Enzyme-Linked Immunosorbent Assay (ELISA) General Protocol.** The plates were coated with the antigens ( $100\text{ }\mu\text{L}/\text{well}$  in coating buffer) overnight at  $4\text{ }^{\circ}\text{C}$  covered with adhesive plate sealers. The day after, the plates were washed four times with PBST ( $300\text{ }\mu\text{L}/\text{well}$ ) and the solutions of the analyte ( $50\text{ }\mu\text{L}/\text{well}$  in PBST; zero analyte is only PBST) and/or the antisera ( $50\text{ }\mu\text{L}/\text{well}$  in PBST,  $100\text{ }\mu\text{L}/\text{well}$  for the noncompetitive assays) were added and incubated for 30 min at room temperature (RT). The plates were washed again as before, and a solution of antiIgG-HRP (1/6000 in PBST) was added to the wells ( $100\text{ }\mu\text{L}/\text{well}$ ) and incubated for 30 min more at RT. The plates were washed again, and the substrate solution was added ( $100\text{ }\mu\text{L}/\text{well}$ ). Color development was stopped after 30 min at RT with  $4\text{ N H}_2\text{SO}_4$  ( $50\text{ }\mu\text{L}/\text{well}$ ), and the absorbances were read at 450 nm.

Noncompetitive indirect ELISA was used for the screening of the avidity of the 13 antisera obtained vs the 69 coating antigens by measuring the binding of serial dilutions (1/1000 to 1/64 000) of each antisera to the microtiter plates coated with different dilutions ( $10\text{ }\mu\text{g mL}^{-1}$  to  $9\text{ ng mL}^{-1}$ ) of each of the BSA, CONA, and OVA conjugates. From these experiments, optimum concentrations for coating antigens and antisera dilutions were chosen to produce around 0.7–1 units of absorbance in 30 min.

**Competitive Indirect ELISAs.** The avidity of 2,4,6-TCA to compete with the different coating antigens for the antibody binding was investigated by adding 12 serial dilutions of the analyte ( $10\text{ }000\text{ nM}$  to  $1\text{ pM}$ , in PBST,  $50\text{ }\mu\text{L}/\text{well}$ ) to the coated plates followed by the appropriately diluted As ( $50\text{ }\mu\text{L}/\text{well}$ ). The mixture was incubated for 30 min, and the plates were then processed as described above. The standard curve was fitted to a four parameter equation according to the following formula:  $Y = [(A - B)/1 - (x/C)^D] + B$ , where  $A$  is the maximal absorbance,  $B$  is the minimum absorbance,  $C$  is the concentration producing 50% of the maximal absorbance, and  $D$  is the slope at the inflection point of the sigmoid curve.

## RESULTS AND DISCUSSION

**Hapten Design.** Four different chemical structures were initially contemplated as potential immunizing haptens to raise antibodies against TCA (see **Figure 2**, top). Hapten **A** with the spacer arm at the *meta* position preserved the three chlorine atoms and the methoxy group, but the introduction of the alkyl in the aromatic ring could affect its electronic properties. In hapten **B**, the methoxy group was replaced by the spacer arm but the rest of the molecule remained unchanged. In contrast, the chemical structures of the haptens **C** and **D** had substituted one of the chlorine atoms by the spacer arms at either the *para* or the *ortho* position, respectively. From these last two potential haptens, hapten **C** maximized the exposure to the immune system of the area defined by the methoxy group and the two chlorine atoms in *ortho*, which appeared as one of the most important epitopes.

Theoretical models and calculations have proven to be useful tools to predict the suitability of a particular chemical structure as immunizing hapten to raise antibodies against a nonimmunogenic compound such as TCA (34, 36–38). Therefore, by analyzing the features of these molecules at their minimum energetic levels according to MNDO and PM3 models, it was expected to obtain more objective data. One of the criteria studied was the electronic distribution. According to it, small differences could be observed in the punctual charges of the aromatic rings as shown in **Figure 3**. Hapten **A** followed the same pattern of electronic distribution as TCA although the total charge was more negative, mainly because of the less positive charges at the *meta* positions produced by the introduction of the spacer arm in one of them. In contrast, if the spacer arm was introduced instead of the methoxy group, like in hapten **B**, the electronic resemblance to the analyte, regarding punctual charges in the aromatic ring, was complete. From this point of view, haptens **C** and **D** showed greater differences. The positions lacking the chlorine atom were in these haptens much more positive, and as a result, the overall charge was significantly less negative for these haptens (see **Figure 3**, right bars). Thus, considering electronic distribution, hapten **B** better mimicked the behavior of the analyte. However, we also have to consider

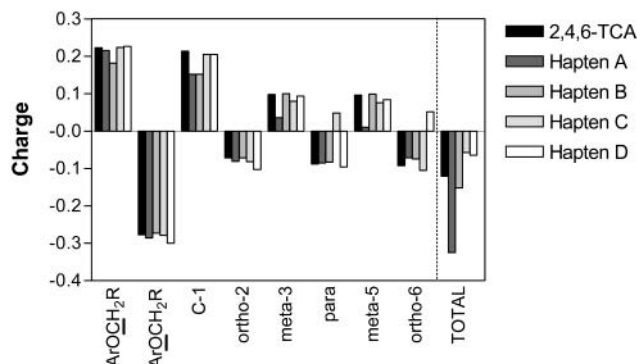


**Figure 3.** Graph showing the punctual charges calculated at their minimum energetic level using MNDO molecular models. Calculations have been made using the corresponding amide derivatives to mimic the conjugated haptens. R is H for TCA and haptens A, C, and D. R is  $(\text{CH}_2)_3\text{CONH}_2$  for hapten B.

the effect that the introduction of the spacer arm could provoke the spatial conformation of these molecules. Attending to this aspect, while in the TCA molecule, the methoxy group appeared placed in the same plane as the one defined by the aromatic ring (see **Figure 2**, bottom); haptens A and B showed a different geometry since the alkyloxy group had the tendency to move away from this plane. In contrast, the geometry of the analyte was better preserved in haptens C and D, which showed the same behavior as the target analyte.

These results made the selection of the most suitable immunizing hapten difficult. Despite the greater electronic similarity of hapten B, we were concerned about a possible drop in the avidity of the antisera if this hapten was used, especially considering the change in the geometry of the alkyloxy group evidenced by the molecular models. The geometry of haptens C and D was similar to that of TCA, but the absence of one of the chlorine atoms was also worrying. From these two haptens, hapten C was preferred since it orientated better to the immune system, recognition of the area defined by the methoxy group and the chlorine atoms in *ortho*. On the other hand, regardless of the small changes in the electronic distribution, hapten A was the only hapten preserving entirely the functional groups of the target analyte. Consequently, we decided to assess the results obtained from the theoretical models by raising antibodies against the three haptens A, B, and C. The features of the resulting immunoassays could help us to know which parameter has more influence on the antibody qualities in addition to providing a battery of antibodies with different properties.

**Synthesis of the Haptens.** Hapten A was prepared forming the anisole of the methyl 3-(3-hydroxy-2,4,6-trichlorophenyl)propanoate (36) using methyl iodide in the presence of dry  $\text{K}_2\text{CO}_3$ . The hydrolysis of the resulting methyl ester gave hapten A with a 67% global yield. Hapten B was obtained in only two steps from 2,4,6-TCP by O-alkylation through a nucleophilic substitution of a  $\omega$ -halogenated alcanoic acid by the phenoxy group generated in basic media. The hydrolysis of the ester 5 afforded the desired hapten on a 46% global yield. Finally, hapten C was prepared as hapten A with a 51% yield by substituting and first forming the methyl ether of methyl-3-(3,5-dichloro-4-hydroxyphenyl)propanoate (41) and hydrolyzing the methyl ester (see **Figure 4**).

Some competitive immunoassays work better under heterogeneous conditions (45, 46). This means that the chemical structure of the hapten used as the competitor is slightly different from that of the immunizing hapten and therefore different to that of the analyte. The theoretical idea is to favor binding of

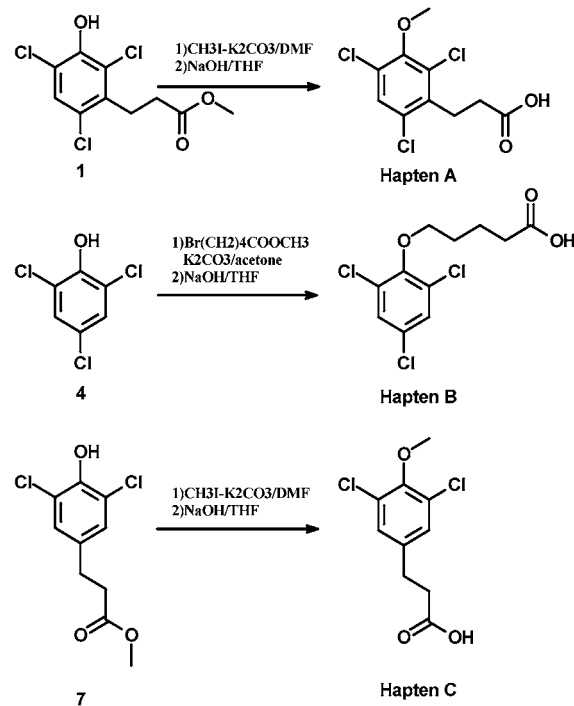


**Figure 4.** Synthetic pathways used for the preparation of the immunizing haptens A–C. The synthesis of the starting materials 1 and 7 had already been reported in our group by Galve and co-workers (36, 47).

the antibodies to the analyte, even if present only at the trace level, by diminishing the affinity of the antibodies vs the competitor (28, 33, 34, 46). Thus, taking advantage of the battery of phenolic compounds previously synthesized in our group (36, 37, 41), a new set was prepared by selecting some of them and converting them to the corresponding anisoles following the same procedure applied for hapten A (see **Figure 1** for chemical structures).

**Antibody Production.** Haptens A, B, and C were conjugated to KLH and BSA following the AE method. The coupling reactions were verified by analyzing the BSA derivatives by MALDI-TOF-MS and comparing the observed molecular weight with that of the intact protein. An average of 21, 38, and seven haptens covalently attached to each molecule of BSA was estimated for the conjugates A-BSA (AE), B-BSA (AE), and C-BSA (AE), respectively. Three rabbits were inoculated with each immunogen using 100  $\mu\text{g}$  of the corresponding hemocyanin conjugate (A-KLH, B-KLH, and C-KLH) and boosted each month for 6 months until no significant increase in the antibody titer was observed. The antisera obtained from immunizing with A-KLH were named As74, As75, and As76. The antisera As77, As78, and As79 were the antisera obtained from the three rabbits immunized with B-KLH. Finally, from immunizing with C-KLH, the antisera identified as As88, As89, and As90 were produced.

**Screening of the Antiserum Avidity for the Immunoagents.** At the first instance, the avidity of the antisera vs the battery of competitors (C9, C10, C12, C18–C20, and C22 coupled to BSA, CONA, and OVA by the MA conjugation method) was tested on a simple experiment by measuring the binding of serial dilutions of the antisera to plates coated with the coating antigens at 1  $\mu\text{g L}^{-1}$  (see **Table 1**). The antisera against A-KLH showed a broad recognition of most of the chemical structures tested as competitors. The highest avidity was observed for those coating antigens with an ether group (e.g., C1–C4, C9, C22, and haptens B and C) instead of a

Table 1. Relative Avidities<sup>a</sup> of the Antisera Raised against TCA vs the Battery of Competitor Haptens

Antigens	Antisera								
	A-KLH			B-KLH			C-KLH		
	As74	As75	As76	As77	As78	As79	As88	As89	As90
C1-BSA									
C1-CONA									
C1-OVA									
C2-BSA									
C3-BSA									
C3-CONA									
C3-OVA									
C4-BSA									
C4-CONA									
C4-OVA									
C7-BSA									
C9-BSA									
C9-CONA									
C9-OVA									
A-BSA									
A-CONA									
A-OVA									
C14-CONA									
C-BSA									
C-CONA									
C-OVA									
C19-OVA									
C22-BSA									
C22-CONA									
C22-OVA									
B-BSA									
B-CONA									
B-OVA									

Absorbance

1.5  
0.7-1.5  
0.4-0.7  
>0.4

<sup>a</sup> The relative avidities have been expressed as the absorbance obtained when measuring the binding of the antisera 1/1000 times diluted in PBST to microplates coated with the antigens at a concentration of 1  $\mu\text{g mL}^{-1}$ . See the legend in the right part of the table for the meaning of the shadow boxes.

hydroxyl group. Thus, haptens C6 or C5 were not recognized at all, while C7 and C14 were only slightly recognized (see chemical structures on Figure 1). In contrast to these results, the antisera obtained against immunogens B-KLH and C-KLH showed a very narrow avidity and the titers observed were also lower. Thus, As77–79 raised against B-KLH only recognized the competitors C1 and C9. The recognition of hapten C1 was expected since it only differed from hapten B in the length of the spacer arm. From the antisera against C-KLH, As88 showed a different behavior from As89 and As90, which gave very low responses for most of the antigens. Nevertheless, As88 only recognized those coating antigens containing haptens possessing a high degree of homology with the immunizing haptens such as haptens B, C, and C1 (see Table 1).

**Effect of the Immunizing Hapten on the Immunoassay Properties.** Those As/coating antigen combinations showing acceptable titers were used to assess the ability of the analyte to displace the equilibrium, after establishing the appropriate concentration of each immunoreagent by two-dimensional checkerboard titration experiments. Table 2 shows the features of the indirect ELISAs obtained that exhibited adequate characteristics ( $A_{\text{max}}$  0.5–1.2 units of absorbance, slope > 0.5, signal-to-noise ratio > 5) and  $\text{IC}_{50}$  values lower than 10  $\mu\text{g L}^{-1}$ . The most noticeable result was that despite the low avidity shown for the competitors, the antisera obtained against hapten C gave the greater number of competitive immunoassays with acceptable features. It must be noticed that these are the results obtained from the screening using the standard protocol described in the Experimental Section. It is possible to think

Table 2. Features of the Best Competitive Assays Obtained with the Antisera Raised against the Three Immunizing Haptens<sup>a</sup>

immunogen	As/antigen	$A_{\text{max}}$	$A_{\text{min}}$	slope	$\text{IC}_{50}$ ( $\mu\text{g L}^{-1}$ )	$R^2$
A-KLH	As76/C3-OVA	0.950	0.038	-0.49	3.18	0.980
	As76/C14-CONA	1.129	0.076	-0.51	2.29	0.980
B-KLH	As78/C9-OVA	1.600	0.328	-0.80	9.73	0.980
C-KLH	As88/C1-CONA	0.620	0.004	-0.61	4.82	0.980
	As88/C-BSA	1.054	0.029	-0.95	5.84	0.995
	As88/C-CONA	0.648	0.007	-0.91	0.21	0.995
	As88/C-OVA	0.618	0.017	-0.92	0.19	0.991
	As88/B-CONA	0.517	0.014	-1.25	5.73	0.990
	As88/B-OVA	0.500	0.010	-1.61	6.93	0.980

<sup>a</sup> Only those assays showing acceptable features were selected for further investigation ( $A_{\text{max}}$  0.5–1.2 units of absorbance, slope > 0.5, signal-to-noise ratio > 5) and  $\text{IC}_{50}$  values lower than 10  $\mu\text{g L}^{-1}$ .

that by changing the experimental conditions and the physico-chemical features (ionic strength, pH, incubation times, etc.) other combinations could have rendered usable assays. This could be especially probable for the antibodies raised against hapten A, in light of the great number of competitors that were recognized by these antibodies.

## CONCLUSIONS

Electronic distribution and geometry are objective criteria to assist immunizing hapten design although it is not always clear which parameter will have a greater influence on the antibody

properties. Thus, while evaluating several immunizing haptens to raise antibodies against the antifouling agent Irgarol 1051, the participation of hydrophobic interactions with the area defined by the *tert*-butyl group present in this molecule appeared to be quite important (34). In contrast, producing antibodies against 2,4,6- and 2,4,5-TCP, the electronic distribution played a major role, especially considering the change in the electronic charge occurring at certain pH values of the media (36, 38). The results obtained now for the case of TCA seem to indicate that the geometry of the immunizing hapten is a very important parameter. Thus, hapten C produced the highest number of competitive immunoassays with acceptable features indicating that their ability to bind the analyte is higher than that for the antibodies raised against haptens A and B. As we mentioned before, the methoxy group is displayed in hapten C on identical conformation as in the analyte. However, we must also remark that hapten C directs recognition of immune system vs the more characteristic moiety of the molecule formed by the methoxy group and the two chlorine atoms in *ortho*. On the other hand, the electronic distribution of hapten C only differs from that of the analyte in the punctual charge at the *para* position, but this part is the one less exposed to the immune system due to the steric hindrance caused by the carrier protein. It seems thus that the effect produced by the introduction of the spacer arm in the electronic distribution of a molecule should be evaluated taking into account other factors such as the participation of the moiety affected on the formation and stabilization of the antibody-analyte complex. However, we must not forget that detectability is only one of the aspects that defines an immunoassay. On the other hand, in spite of the fact that the antibody is the key reagent of any immunochemical technique, the features of the other immunoreagents (e.g., coating antigen, analyte) also have an influence on the robustness of the analytical method. Therefore, further studies will be addressed to evaluate these immunoreagents and their effect on other immunoassay features of these competitive immunoassays such as reproducibility, accuracy, selectivity, etc.

**Supporting Information Available:** Procedures and spectral data for haptens C9, C10, C12, C18–C20, and C22. Results obtained from the characterization of the hapten–BSA conjugates by MALDI-TOF-MS. This material is available free of charge via the Internet at <http://pubs.acs.org>.

## LITERATURE CITED

- Tanner, H. Z. C.; Buser, H. R. 2,4,6-trichloroanisole: eine dominierend Komponente des Korkgeschmacks. *Schweiz. Z. Obst. Weinbau* **1981**, *117*, 97–103.
- Amon, J. M.; Vandepier, J. M.; Simpson, R. F. Compounds responsible for cork taint in wine. *Aust. N. Z. Wine Ind. J.* **1989**, *62*–69.
- Chatonnet, P.; Guimberteau, G.; Dubourdieu, D.; Boidron, J. N. Nature et origine des odeurs de moisi dans les caves incidence sur la contamination des vins. *J. Int. Sci. Vigne Vin* **1994**, *28*, 131–151.
- Fuller, P. Cork Taint: Closing in on an Industry Problem. *Aust. N. Z. Wine Ind. J.* **1995**, *10*, 58–60.
- Pollnitz, A. P.; Pardon, K. H.; Liacopoulos, D.; Skouroumounis, G. K.; Sefton, M. A. The analysis of 2,4,6-trichloroanisole and other chloroanisoles in tainted wines and corks. *Aust. J. Grape Wine Res.* **1996**, *2*, 184–190.
- Maarse, H. N.; Angelino, L. M.; S. A. G. F. *Proceedings of the Second Wartburg Aroma Symposium*, Wartburg.
- Suárez, J. A.; Navascués, F.; J. C.; Vila, B.; Colomo, C.; García-Vallejo. Présence de champignons et concentration de chloroanisoles pendant le processus de fabrication des bouchons de liège pour l'embouteillage des vins. *Bull. I. V.* **1997**, 793–794.
- Lefebvre, A.; Riboulet, J. M.; Boidron, J. N.; Ribéreau-Gayon, P. Incidence des microorganismes du liège sur les altérations olfactives du vin. *Sci. Aliments* **1983**, *3*, 265–278.
- Dubois, P.; Rigaud, J. The taste of stoppers [in wine]. *Sem. Vitivinic.* **1981**, *36*, 4433–4434.
- Buser, H. R.; Zanier, C.; Tanner, H. Identification of 2,4,6-trichloroanisole as a potent compound causing cork taint in wine. *J. Agric. Food Chem.* **1982**, *30*, 359–362.
- Ahlborg, U. G.; Thunberg, T. M. Chlorinated phenols: occurrence, toxicity, metabolism and environmental impact. In *CRC Crit. Rev. Toxicol.* **1980**, 1–35.
- Nyström, A.; Grimvall, A.; Krantz-Rülcker, C.; Sävenhed, R.; Akerstrand, K. Drinking Water off-Flavour caused by 2,4,6-Trichloroanisole. *Water Sci. Technol.* **1992**, *25*, 241–249.
- Jensen, S. E.; Anders, C. L.; Goatcher, L. J.; Perley, T.; Kenefick, S.; Hruday, S. E. Actinomycetes as a Factor in Odor Problems affecting Drinking Water from North Saskatchewan River. *Water Res.* **1994**, *28*, 1393–1401.
- Kim, Y.; Lee, Y.; Gee, C.; Choi, E. Treatment of Taste and Odor Causing Substances in Drinking Water. *Water Sci. Technol.* **1997**, *35*, 29–36.
- Whitfield, F. B.; McBride, R. L.; Nguyen, T. H. L. Flavour Perception of Chloroanisoles in Water and Selected Processed Foods. *J. Sci. Food Agric.* **1987**, *40*, 357–365.
- Cantagrel, R.; Vidal, J. P. *Proceedings of the 6th International Flavour Conference*, Rethymnon, Crete; Elsevier Scientific Publishers: Amsterdam; pp 139–157.
- Bertrand, A.; Barrios, M. L. Stopper contamination byproducts used in the treatment of bottle storage pallets. *Rev. Fr. Oenol.* **1994**, *149*, 29–32.
- Whitfield, F. B.; Kevin, J. S.; Ly Nguyen, T. H. Simultaneous Determination of 2,4,6-Trichloroanisole, 2,3,4,6-Tetrachloroanisole and Pentachloroanisole in Foods and Packaging Materials by High-Resolution Gas Chromatography-Multiple Ion Monitoring-Mass Spectrometry. *J. Sci. Food Agric.* **1986**, *37*, 85–96.
- Evans, T. J.; Butzke, C. E.; Ebeler, S. E. Analysis of 2,4,6-trichloroanisole in wines using solid-phase extraction coupled to gas chromatography–mass spectrometry. *J. Chromatogr. A* **1997**, *786*, 293–298.
- Fischer, C.; Fischer, U. Analysis of cork taint in wine and cork material at olfactory subthreshold levels by solid-phase microextraction. *J. Agric. Food Chem.* **1997**, *45*, 1995–1997.
- Taylor, M. K.; Young, T. M.; Butzke, C. E.; Ebeler, S. E. Supercritical Fluid Extraction of 2,4,6-Trichloroanisole from Cork Stoppers. *J. Agric. Food Chem.* **2000**, *48*, 2208–2211.
- Marco, M.-P.; Gee, S.; Hammock, B. D. Immunochemical techniques for environmental analysis. I. Antibody production and immunoassay development. *Trends Anal. Chem.* **1995**, *14*, 415–425.
- Gabalton, J. A.; Maquieira, A.; Puchades, R. Current trends in immunoassay-based kits for pesticide analysis. *Crit. Rev. Food Sci. Nutr.* **1999**, *39*, 519–538.
- Fitzpatrick, J.; Fanning, L.; Hearty, S.; Leonard, P.; Manning, B. M.; Quinn, J. G.; O'Kennedy, R. Applications and recent developments in the use of antibodies for analysis. *Anal. Lett.* **2000**, *33*, 2563–2609.
- Harris, A. S.; Wengatz, I.; Wortberg, M.; Kreissig, S. B.; Gee, S. J.; Hammock, B. D. Development and application of immunoassays for biological and environmental monitoring. *Mult. Stresses Ecosyst.* **1998**, 135–153.
- Tang, Z.; Karnes, H. T. Coupling immunoassays with chromatographic separation techniques. *Biomed. Chromatogr.* **2000**, *14*, 442–449.
- Sherry, J. Environmental immunoassays and other bioanalytical methods: overview and update. *Chemosphere* **1997**, *34*, 1011–1025.

- (28) Oubiña, A.; Ballesteros, B.; Bou-Carrasco, P.; Galve, R.; Gascón, J.; Iglesias, F.; Sanvicens, N.; Marco, M. P. Immunoassays for Environmental Analysis. In *Sample Handling and Trace Analysis of Pollutants*; Barceló, D., Ed.; Elsevier Sciences: Amsterdam, 2000.
- (29) Szurdoki, F.; Bekheit, H. K. M.; Marco, M.-P.; Goodrow, M. H.; Hammock, B. D. Important Factors in Hapten Design and Enzyme-Linked Immunosorbent Assay Development. In *New Frontiers in Agrochemical Immunoassay*; Kurtz, D. A., Skerritt, J. H., Stanker, L., Eds.; AOAC International: Arlington, VA, 1995; pp 39–63.
- (30) Skerritt, J. H.; Lee, N. Approaches to the synthesis of haptens for immunoassay of organophosphate and synthetic pyrethroid insecticides. *ACS Symp. Ser.* **1996**, 124–149.
- (31) Lawruk, T. S.; Hottesntein, C. S.; Fleeker, J. R.; Rubio, F. M.; Herzog, D. P. Factors influencing the specificity and sensitivity of triazine immunoassays. In *Herbicide Metabolites in Surface Water and Groundwater*; ACS, American Chemical Society: Washington, DC, 1996.
- (32) Goodrow, M. H.; Sanborn, J. R.; Stoutamire, D. W.; Gee, S. J.; Hammock, B. D. Strategies for immunoassay hapten design. In *Immunoanalysis of Agrochemicals. Emerging Technologies*; Nelson, J. O., Karu, A. E., Wong, R. B., Eds.; American Chemical Society: Washington, DC, 1995.
- (33) Carlson, R. E. Hapten versus competitor design strategies for immunoassay development. In *Immunoanalysis for Agrochemicals*; Nelson, J. O., Karu, A. E., Wong, R. B., Eds.; American Chemical Society: Washington, DC, 1995; pp 141–152.
- (34) Ballesteros, B.; Barceló, D.; Sanchez-Baeza, F.; Camps, F.; Marco, M. P. Influence of the hapten design on the development of a competitive ELISA for the determination of the antifouling agent Irgarol 1051 at trace levels. *Anal. Chem.* **1998**, *70*, 4004–4014.
- (35) Lee, N. J.; Skerritt, J. H.; McAdam, D. P. Hapten synthesis and development of ELISAs for detection of endosulfan in water and soil. *J. Agric. Food Chem.* **1995**, *43*, 1730–1739.
- (36) Galve, R.; Camps, F.; Sanchez-Baeza, F.; Marco, M.-P. Development of an Immunochemical Technique for the Analysis of Trichlorophenols Using Theoretical Models. *Anal. Chem.* **2000**, *72*, 2237–2246.
- (37) Galve, R.; Sanchez-Baeza, F.; Camps, F.; Marco, M.-P. Indirect competitive immunoassay for trichlorophenol determination: rational evaluation of the competitor heterology effect. *Anal. Chim. Acta* **2002**, *452*, 191–206.
- (38) Nichkova, M.; Galve, R.; Marco, M.-P. Biological Monitoring of 2,4,5-Trichlorophenol (I): Preparation of antibodies and development of an immunoassay using theoretical models. *Chem. Res. Toxicol.* **2002**, *15*, 1360–1370.
- (39) Dewar, M. J. S.; Thiel, W. Ground States of Molecule. 38. The MNDO Methodol. Approximations and Parameters. *J. Am. Chem. Soc.* **1977**, *99*, 4899–4917.
- (40) Stewart, J. J. P. Optimization of Parameters for Semiempirical Methods. I Methodol. *J. Comput. Chem.* **1989**, *10*, 209–221.
- (41) Galve, R.; Nichkova, M.; Camps, F.; Sanchez-Baeza, F.; Marco, M.-P. Development and Evaluation of an Immunoassay for Biological Monitoring Chlorophenols in Urine as Potential Indicators of Occupational Exposure. *Anal. Chem.* **2002**, *74*, 468–478.
- (42) Gascón, J.; Oubiña, A.; Ballesteros, B.; Barceló, D.; Camps, F.; Marco, M.-P.; González-Martínez, M.-A.; Morais, S.; Puchades, R.; Maquieira, A. Development of a highly sensitive enzyme-linked immunosorbent assay for Atrazine. Performance evaluation by flow-injection immunoassay. *Anal. Chim. Acta* **1997**, *347*, 149–162.
- (43) Marco, M.-P.; Hammock, B. D.; Kurth, M. J. Hapten design and development of an ELISA (enzyme-linked immunosorbent assay) for the detection of the mercapturic acid conjugates of naphthalene. *J. Org. Chem.* **1993**, *58*, 7548–7556.
- (44) Ballesteros, B.; Barceló, D.; Camps, F.; Marco, M. P. Enzyme-Linked Immunosorbent Assay for the Determination of the Antifouling Agent Irgarol 1051. *Anal. Chim. Acta* **1997**, *347*, 139–147.
- (45) Schneider, P.; Goodrow, M. H.; Gee, S. J.; Hammock, B. D. A highly sensitive and rapid ELISA for the arylurea herbicides diuron, Monuron, and linuron. *J. Agric. Food Chem.* **1994**, *42*, 413–422.
- (46) Abad, A.; Moreno, M. J.; Montoya, A. Hapten synthesis and production of monoclonal antibodies to the *N*-methylcarbamate pesticide methiocarb. *J. Agric. Food Chem.* **1998**, *46*, 2417–2426.

---

Received for review January 2, 2003. Revised manuscript received May 6, 2003. Accepted May 8, 2003. This work has been supported by INIA (VIN00-053-C3-2), the EC Quality of Life Program (Contract QLRT-2000-01670), and CICYT (AGL2001-5005-E and AGL2002-04635-C04-03).

JF034003H